Journal of Cleaner Production 70 (2014) 145–153

Contents lists available at ScienceDirect

Journal of Cleaner Production

journal homepage: www.elsevier.com/locate/jclepro

Municipal solid waste conversion to transportation fuels: a life-cycle estimation of global warming potential and energy consumption

Phillip N. Pressley [a,*], Tarek N. Aziz [a], Joseph F. DeCarolis [a], Morton A. Barlaz [a], Feng He [b], Fanxing Li [b], Anders Damgaard [c]

[a] Department of Civil, Construction, and Environmental Engineering, NC State University, 2501 Stinson Drive, Raleigh, NC 27695, USA
[b] Department of Chemical and Biomolecular Engineering, NC State University, 911 Partners Way, Raleigh, NC 27695, USA
[c] Department of Environmental Engineering, Technical University of Denmark, Miljøvej, 2800 Kongens Lyngby, Denmark

ARTICLE INFO

Article history:
Received 5 July 2013
Received in revised form
13 February 2014
Accepted 15 February 2014
Available online 25 February 2014

Keywords:
Municipal solid waste
Gasification
Fischer-Tropsch
Life cycle assessment
Liquid fuels

ABSTRACT

This paper utilizes life cycle assessment (LCA) methodology to evaluate the conversion of U.S. municipal solid waste (MSW) to liquid transportation fuels via gasification and Fischer-Tropsch (FT). The model estimates the cumulative energy demand and global warming potential (GWP) associated with the conversion of 1 Mg (1 Mg = 1000 kg) of MSW delivered to the front gate of a refuse-derived fuel (RDF) facility into liquid transportation fuels. In addition, net energy production is reported to quantify system performance. The system is expanded to include substituted electricity and fuel. Under a set of default assumptions, the model estimates that 1 Mg of MSW entering the RDF facility yields 123 L of gasoline, 57 L of diesel, 79 kg of other FT products, and 193 kWh of gross electricity production. For each Mg of MSW, the conversion process consumes 4.4 GJ of primary energy while creating fuels and electricity with a cumulative energy content of 10.8 GJ. Across a range of waste compositions, the liquid fuels produced by gasification and FT processing resulted in a net GWP ranging from −267 to −144 kg CO_2e per Mg MSW, including offsets for conventional electricity and fuel production. The energy requirement associated with syngas compression for FT processing was significant and resulted in high levels of process-related GWP. The model demonstrates that an increased biogenic MSW fraction, assumed to be carbon neutral, reduced the GWP. However, a greater GWP reduction could be obtained through reduced FT pressure requirements, increased gas reaction rates, or a less carbon intensive power mix.

© 2014 Elsevier Ltd. All rights reserved.

1. Introduction

Interest in clean, affordable energy and diversion of waste from landfills drives interest in energy recovery from municipal solid waste (MSW). As an energy feedstock, MSW is abundant and waste producers typically pay tipping fees for disposal of the 260 million tons produced annually in the U.S. (U.S. EPA, 2011). Many energy recovery options from solid waste exist, including landfill gas-to-energy, incineration, anaerobic digestion, and gasification. Life cycle assessment (LCA) can be employed to evaluate the relative energy and environmental performance of such options from curb to ultimate disposal, yielding insights that inform public policy and investment decisions (e.g., Kaplan et al., 2009; Levis and Barlaz, 2011).

LCA has previously been used to characterize the environmental performance of energy recovery options from MSW by accounting for all process-related energy and emissions, both direct and indirect. For example, landfill gas-to-energy studies include emissions associated with curbside collection processes, fugitive methane, electricity generation, and heavy machine operation (Ménard et al., 2004; Kaplan et al., 2009; Levis and Barlaz, 2011). Waste-to-energy studies account for emissions associated with curbside collection processes, energy use, electricity generation, and ash management (Harrison et al., 2000; Riber et al., 2008; Koehler et al., 2011). Other options for energy recovery from solid waste exist, including conventional gasification, torrefaction, pyrolysis, and plasma arc gasification, but scarce operational data has limited the evaluation of their life cycle impacts.

This paper utilizes LCA methodology to evaluate the conversion of an MSW-derived feedstock into a liquid hydrocarbon, similar to crude oil, via gasification and Fischer-Tropsch (FT). A unique feature of the gasification-FT (GFT) pathway – relative to many other MSW

---

* Corresponding author. Tel.: +1 919 515 2331; fax: +1 919 515 7908.
E-mail address: pnpressl@ncsu.edu (P.N. Pressley).

http://dx.doi.org/10.1016/j.jclepro.2014.02.041
0959-6526/© 2014 Elsevier Ltd. All rights reserved.

energy recovery options, which ultimately produce electricity – is that it produces a set of liquid transportation fuels. Gasification thermochemically converts a solid feedstock into a synthesis gas (i.e., syngas), which is primarily comprised of carbon monoxide, diatomic hydrogen, and carbon dioxide (Lee et al., 2007). Syngas is then passed over an iron- or cobalt-based catalyst in a FT reactor (Spath and Dayton, 2003). The resultant synthetic crude oil (i.e., syncrude) represents an energy commodity that can be processed in an existing petroleum refinery into liquid transportation fuels and chemical co-products. Several commercial and governmental entities have pursued commercial MSW gasification over the last decade (Pytlar, 2010), and full-scale FT technology is currently used to create liquid transportation fuels from coal (Cao et al., 2008). The gasification of several MSW components has been demonstrated experimentally (Ahmed and Gupta, 2009; Gai and Dong, 2012), but it has never been combined with FT technology in a commercial application.

Though full-scale gasification and FT demonstrations have been limited, many computer models simulate the chemical reactions within gasifiers and FT reactors. Thermodynamic equilibrium models can predict syngas yield and composition from gasifiers (Vera et al., 2013; Shabbar and Janajreh, 2013; Sreejith et al., 2012; Arafat and Jijakli, 2013); however, many require process expertise and utilize complex proprietary software, such as ASPEN Plus (2010) or Cyclo-Tempo (2012), which limit their application within LCA. While such thermodynamic equilibrium models can estimate gasification and FT yields, simple and transparent models that can quickly respond to changes in input assumptions are often better suited for use within an LCA framework. Also, once developed, simplified LCA models can avoid the need for proprietary software or process expertise. Models have been developed to estimate syngas yield (Fock et al., 2000) and FT product distribution (Flory, 1936), but no existing simplified process models predict both syngas composition and FT fuel yield for use in building LCA inventories.

While LCA has been used to evaluate the environmental performance of biomass gasification processes (Carpentieri et al., 2005), plasma gasification of construction and demolition waste as well as forest residuals (Nuss et al., 2013), and biomass conversion to transportation fuel technologies, including FT (Swain et al., 2011), there has been limited LCA work to evaluate the use of gasification for conversion of MSW to liquid fuels. RTI (2012) conducted an LCA that estimated environmental impacts associated with fuel production from plastic waste; however, they did not include the processing required to convert MSW into the plastic gasifier feedstock. Khoo (2009) quantified the life cycle impacts of MSW gasification, including pre-processing, but the study does not include the downstream use of syngas. Nuss et al. (2012) examined a gasification and FT process that uses MSW as a feedstock, but the target products were plastics.

The goal of this paper is to fill a critical gap in the literature by using LCA methodology (ISO, 2006a,b) to quantify the cumulative energy demand (CED) and global warming potential (GWP) associated with the conversion of as-generated MSW to refined fuel products via GFT. While not an LCA impact category, we also report the net energy production in order to compare the amount of energy produced with the energy required to process the waste. Reflecting this goal, the system boundary ranges from the front gate of the refuse-derived fuel (RDF) facility through fuel combustion. This LCA and the underlying data are focused on application within the U.S. The resultant LCI data and analysis can be used in LCA studies with broader system boundaries aimed at comparing different waste management alternatives.

To conduct this LCA, we developed a spreadsheet model that aggregates the process-related emissions from waste preparation and separation through gasification, FT fuel generation, and fuel utilization. A key challenge was the development of a simplified model appropriate for LCA that predicts the syngas and syncrude compositions based on calibration to complex chemical equilibrium models associated with gasification and FT. The model results include mass flows between each process within the system boundary and the associated CED and GWP as well as net energy production. Model sensitivity to MSW composition and key model input parameters is also explored.

2. Methodology

The functional unit in this LCA is 1 Mg (Mg = metric ton) of mixed waste delivered to a sorting facility that mechanically sorts incoming MSW to produce a refuse-derived fuel (RDF) suitable for a gasifier. As shown in Fig. 1, the following processes are included within the system boundary of this LCA: MSW processing within the RDF facility, gasification, FT, refinery processing, refined product combustion as well as the transportation of RDF and syncrude to downstream destinations.

MSW is mechanically processed into a high calorific RDF fraction with a low moisture content. RDF is fed into a gasifier where thermochemical processing transforms it into a mixture of carbon monoxide (CO), diatomic hydrogen (H_2), carbon dioxide (CO_2), and methane (CH_4), which constitute the syngas (Lee et al., 2007). The resultant syngas is pressurized and purified to remove contaminants harmful to downstream processes, and then processed through FT reactors, where CO and H_2 are converted into longer chain liquid hydrocarbons (Spath and Dayton, 2003). The liquid portion forms syncrude, a mixture of hydrocarbons similar to crude oil. The lighter fractions, such as methane, are combusted on-site to generate electricity. Syncrude is transported from the FT facility to an oil refinery, which produces gasoline, diesel, and other refined products. The combustion of refined products derived from syncrude is considered within the system boundary to account for its GWP relative to petroleum-derived crude oil. An avoided burden approach (European Commission, 2010) is utilized, which credits the system by subtracting the GWP associated with the production and combustion of an equivalent amount of petroleum-derived fuel to that produced from the investigated system.

The LCA spreadsheet model developed for this analysis uses a process-based LCA approach to aggregate the consumption and production of energy and greenhouse gas emissions associated with each process in Fig. 1. We do not use LCA software, but rather draw data from existing LCA databases such as Ecoinvent (2010) and NREL (2012), and manually apply the data within our spreadsheet model. The associated data sources are listed in Appendix A (Table A1). The LCA is carried out as an attributional LCA, as the focus is on the conversion process and not the whole waste management system. As a result, we do not attempt to investigate the consequences of utilizing gasification for other MSW treatment systems. The LCA therefore applies average data sources used in the market in accordance with ISO 14044 (2006b) and ILCD (Situation C1; European Commission, 2010).

Inter-facility transportation emissions are included, since the RDF facility, GFT units, and the refinery are unlikely to be co-located. The modeled transportation modes and corresponding distances are provided in Table A2. We examined a case in which all waste disposal occurs in Raleigh, NC, USA, but transportation to the refinery requires truck transport to a coastal port in Wilmington, NC, USA followed by shipping via tanker to Galveston, TX, USA. Because existing U.S. refinery locations and capacity are limited, we deliberately chose a relatively long transportation distance between the GFT facility and the oil refinery.

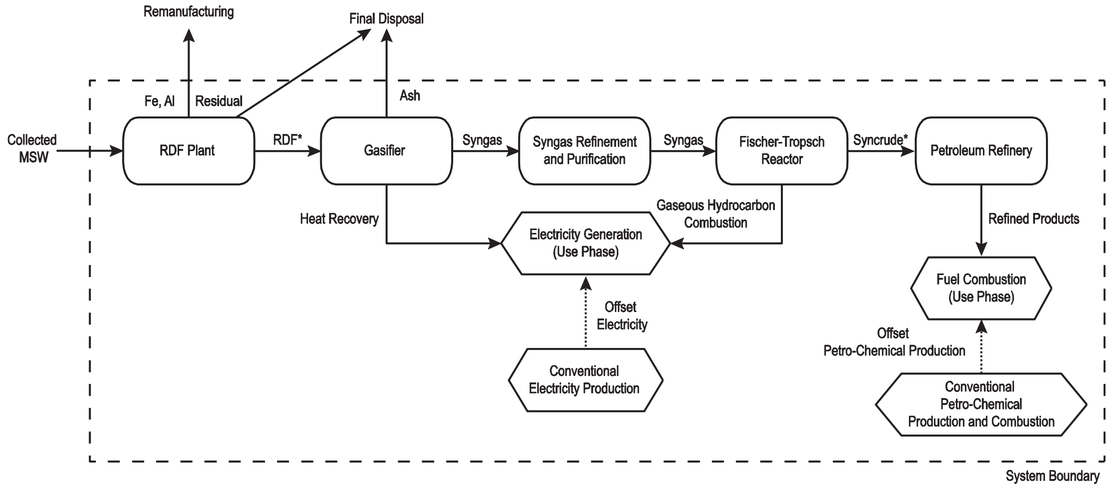
Remanufacturing
Final Disposal
Fe, Al
Residual
Ash
Collected MSW
RDF Plant
RDF*
Gasifier
Syngas
Syngas Refinement and Purification
Syngas
Fischer-Tropsch Reactor
Syncrude*
Petroleum Refinery
Heat Recovery
Electricity Generation (Use Phase)
Gaseous Hydrocarbon Combustion
Refined Products
Fuel Combustion (Use Phase)
Offset Electricity
Offset Petro-Chemical Production
Conventional Electricity Production
Conventional Petro-Chemical Production and Combustion
System Boundary

Fig. 1. High-level mass flow diagram. MSW is mechanically sorted to create RDF, which is treated via the gasification and FT processes to produce liquid fuels. Fuel combustion is included within the system boundary to capture the GWP benefits associated with the biogenic fraction of RDF. Transportation is included for materials followed by (*). Combustion of MSW-derived fuels and the substituted conventional fuels are represented by hexagons.

The impacts of interest are total energy consumption and GWP. Energy and GWP results are presented per functional unit, which allows us to avoid the allocation of environmental burdens among specific waste fractions or refined products. To assess energy consumption, we used cumulative energy demand (CED) (Hirst, 1974), which accounts for all primary energy uses, including any upstream conversion losses. The final system thus accounts for greenhouse emissions and primary energy use from process-specific energy consumption, fuel combustion, and energy offsets resulting from system expansion. Process-specific energy consumption considered within the system boundary comes from three sources: (1) diesel consumed by rolling stock within the RDF plant; (2) grid electricity consumed by sorting equipment within the RDF facility and by the GFT facility for both the compression of syngas and to meet house load requirements; and (3) fuel to transport RDF to the GFT facility and syncrude from the GFT plant to an existing refinery. To calculate GWP, we use the IPCC (2007) impact factors. The GWP of biogenic CO_2 was considered to be zero, which is consistent with the definition of the system boundary (Muñoz et al., 2012; Christensen et al., 2009). Electricity generation from waste heat recovery and combustion of the gaseous FT products substitutes for the U.S. average grid electricity mix, which reduces the net system GWP.

We note several simplifying assumptions in this LCA. First, the curbside collection of MSW is not included within the system boundary, since collection must take place regardless of the waste management alternative. Second, the system does not include production or consumption of chemicals and catalysts in the gasifier, syngas clean-up system, and FT reactors. Where possible, examination of proxy data for these chemicals and catalysts indicates that their contribution to CED and GWP is negligible, and we therefore omit them from this LCA. For example, using a ferrous alloy from Ecoinvent (2010) as a proxy for the iron-based catalyst, the energy consumption and greenhouse gas emissions associated with catalyst production are less than 1% of CED and GWP and well within the uncertainty of the model. Third, we do not include the downstream impacts and potential offsets of remanufacturing and final disposal within the system boundary. While including these processes is relevant when comparing results to other MSW treatment schemes, this study seeks to isolate the environmental impacts associated with the MSW conversion processes. Finally, given the heterogeneity and variability of solid waste, it would be misleading to speculate about the effect of other impact categories in the absence of comprehensive empirical data for syngas contaminants and residual/effluent from pollution control devices. As a result, we only examine CED and GWP in this study.

2.1. Refuse-derived fuel production from MSW

The transformation of MSW to a liquid transportation fuel begins with the delivery of collected waste to an RDF production facility that mechanically sorts the incoming waste, as shown in Fig. 1. MSW processing is included in this analysis because gasification process studies note the benefits of shredding and pelletization of MSW-derived feedstocks on product yield (Ruoppolo et al., 2012; Ammendola et al., 2011), but such processing requires energy use and produces environmental impacts. In this analysis, the RDF facility sorts and processes the delivered MSW, with U.S. national

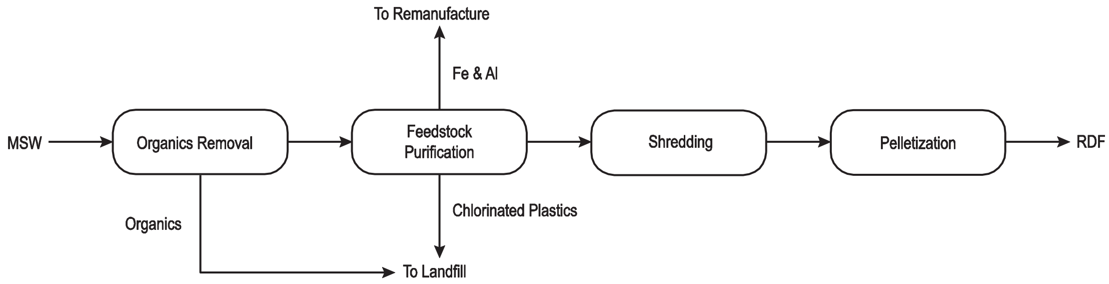

Fig. 2. Conceptual diagram of RDF processing. RDF is created by mechanically removing wet organics (e.g., food and yard waste), metals, and chlorinated plastics, before shredding and pelletizing the remaining material, composed primarily of paper and plastic. A more detailed, process-specific mass flow diagram is provided in Fig. B1 in Appendix B.

Table 1
Required gasifier input parameters. Actual values used in this analysis are presented in Table A4.

Parameters	Range across feedstocks in Table A4		
	Low	High	Unit
Feedstock material properties			
Total volatile solids[a]	93	100	% of total solids
Biogenic carbon content	0	44	% of total solids
Fossil carbon content	0	86	% of total solids
Hydrogen content	4	13	% of total solids
Oxygen content	1	43	% of total solids
Ash content	0	7	% of total solids
Moisture content	6	22	% of total mass
Lower heating value	15.7	43.6	MJ/kg
Gasifier performance parameters			
Air requirement per Mg of feedstock	1.2	5.5	$Mg_{air}/Mg_{feedstock}$
H_2 to CO ratio	0.4	1.5	
CH_4	0	0.3	% of total solids
Total volatile solids unreacted (%)	1	1	% of total solids

[a] Note that biogenic carbon content, fossil carbon content, hydrogen content, and oxygen content are a subset of total volatile solids, but are expressed as % of total solids.

average composition derived from U.S. EPA (2011), as shown in Appendix A (Table A3). To prepare MSW for gasification, the RDF facility removes materials with low-calorific values (e.g., metals, glass), high moisture content (e.g., food waste, yard waste), and process-harmful materials (e.g., polyvinyl chloride) from the input MSW stream (Fig. 2). The remaining waste stream, consisting primarily of paper and plastic, is shredded and pelletized to form RDF that is transported to the gasification facility via heavy-duty truck. A detailed process flow diagram and description of the RDF facility is presented in Appendix B.

The model of RDF production uses MSW composition, equipment energy consumption, and equipment-specific separation efficiencies to calculate the mass of each waste fraction removed by each piece of equipment. These calculated mass flows are combined with equipment-specific throughput capacity factors and energy data to estimate total facility energy consumption. Throughput-based equipment sizing implicitly assumes a linear relationship between throughput and equipment energy consumption, thereby preventing inappropriately sized equipment from biasing results.

2.2. Gasification

The estimated RDF composition, feedstock material properties, and gasifier input parameters are used to calculate syngas composition in the gasification module (Table 1). To achieve the target RDF moisture content of 13.5–22% required for the gasifier, we assume that RDF drying can be achieved with the low grade latent heat generated by the GFT process stream. The quantity of ambient air required per Mg and the H_2 to CO ratio for all feedstock components in this analysis were calculated based on the results of ASPEN Plus simulations of a fluidized bed gasifier operating at 900 °C and 1 atm. Because the syngas yield from gasification is sensitive to the operating temperature, we assume 900 °C, which is consistent with previous studies (Arafat and Jijakli, 2013; Portofino et al., 2013). The key settings and assumptions for the ASPEN Plus simulation model are given in Table 2. For each homogeneous feedstock listed in Table A4, material properties are used along with the assumed 500 Mg per day throughput to estimate syngas yield. The feedstocks were treated as non-conventional components in the ASPEN simulation with heating values from ECN (2012). ASPEN Plus RYield and RGibbs blocks were used to simulate RDF gasification (ASPEN, 2010). In the RYield block, the feedstock is decomposed into its constituent elements (e.g., C, H, O) and inert ash based on the ultimate analysis. The decomposed elements are combined with air and introduced into the RGibbs reactor. The parameters listed in Table 2 were used as constraints. Thermodynamic equilibrium uses the principle of Gibbs free energy minimization and atomic species balances to determine all possible product combinations from the RGibbs block. To estimate compression requirements, a 4 stage compressor with an intercooler was utilized to pressurize syngas to 20 atm. The net heat generation from the gasifier is equal to the heat input from the RYield block minus the sum of the RGibbs block output and the gasifier heat loss, which was assumed to be 1% of the total thermal input (Matuszewsk and Woods, 2012). We estimate that the ancillary (energy) inputs, such as the gasifier bed material, steam, and cooling water amount to ∼1% of the total thermal input heat loss for the gasifier model, which is consistent with Matuszewsk and Woods (2012). As a result, we do not explicitly consider these ancillary inputs. We derived the H_2 to CO ratio and ambient air requirement for each RDF component from the ASPEN Plus simulations for use in the gasifier spreadsheet model.

Table 2
Key assumptions used in the ASPEN Plus simulations of the gasifier.

Property	Value
Ambient condition	$T = 25$ °C, $P = 1$ atm
Air	79% N_2, 21% O_2 by volume
Reaction assumptions	All reactions reach thermodynamic equilibrium
Reactor models	RYield, RGibbs
Property method	PR-BM
Stream class	MIXCINC
Databank	Combust, inorganic, solids, pure
Heat loss in the gasifier	1% of the total thermal input
Compressor specifications	4 stage with intercooler at 40 °C Isentropic efficiency is 0.8 Mechanical efficiency is 1

The gasifier input parameters were used with mass balance equations to estimate syngas yield and composition. The fundamental system mass balance for each waste component i, displayed in Equation (1), shows all mass flowing into the system on the left and all mass leaving the system on the right.

$$m_{air,i} + m_{s,i} + m_i = m_{CO,i} + m_{H_2,i} + m_{CO_2,i} + m_{CH_4,i} + m_{ash,i} + m_{H_2O,i} \quad (1)$$

where:

$m_{air,i}$ mass of air input to gasifier that reacts with waste fraction
$m_{s,i}$ mass of steam that reacts with waste fraction i
m_i mass of waste fraction i input to gasifier
$m_{CO,i}$ mass of CO resulting from gasification of m_i
$m_{H_2,i}$ mass of H_2 resulting from gasification of m_i
$m_{CO_2,i}$ mass of CO_2 resulting from gasification of m_i
$m_{CH_4,i}$ mass of CH_4 resulting from gasification of m_i
$m_{ash,i}$ mass of ash resulting from gasification of m_i
$m_{H_2O,i}$ mass of water resulting from gasification of m_i; unreacted excess steam that exits the gasifier

Syngas yield and composition are calculated independently for each waste component within the RDF. Because each waste component has a specified H_2 to CO ratio, the yield of H_2 and CO also varies by component. The total syngas yield is the summation of each feedstock component's syngas yield. Interactivity between heterogeneous RDF components is not considered because no known analytical method can estimate syngas yield from the interaction of heterogeneous materials (Ahmed et al., 2011), and no empirical data regarding the interaction of all waste components is available. If the H_2 to CO ratio associated with the total syngas yield is lower than the ratio required for effective processing in a FT reactor, the model accounts for the addition of steam to enable the water-gas shift reaction (Marano and Ciferno, 2001). As shown in Equation (2), steam interacts with CO to form H_2 and CO_2 in the water-gas shift reaction:

$$CO + H_2O \rightarrow CO_2 + H_2 \tag{2}$$

The resulting CO_2 is attributed to waste fractions by multiplying the total CO_2 produced through water-gas shift by the fraction of total CO created by the waste fraction. Thus, the CO transformed and steam required by water-gas shift from each waste fraction is proportional to the waste fraction's contribution to total CO. This mass balance approach simplifies the estimation of syngas composition and yield, and neglects feedstock component interactivity, which represents a simplifying assumption that is necessary in the absence of more experimental data.

The results from the spreadsheet model were compared with results from the same ASPEN Plus simulations used to generate the H_2 to CO ratio and air requirement for each RDF component. The spreadsheet model estimated the CO and H_2 yields within 10% of ASPEN Plus for all feedstocks with moisture contents less than 10%, as shown in Appendix C, Tables C1 and C2. In this analysis, we used the ASPEN Plus CH_4 estimates from the simulations where CH_4 production was unconstrained.

2.3. Syngas purification

Syngas exiting a gasifier contains impurities from the feedstock. The composition and quantity of the impurities in syngas from an MSW-fed gasifier are largely unknown, making purification technology selection uncertain (Belgiorno et al., 2003) and preventing accurate estimation of non-energy inputs and wastes. In previous work, energy consumption associated with conventional WTE facility components, including incinerator management technology and air pollution control equipment, was modeled as house load, a single parameter representing facility electricity demand (Harrison et al., 2000). Similarly, in this analysis, a portion of the gasification facility's energy requirements are modeled as a house load, such that the electricity requirements of gasification monitoring equipment and syngas purification technology are denoted as 2% of the feedstock energy content on an LHV basis, consistent with Harrison et al. (2000). The house load does not include energy associated with the compressor used to give the syngas a CO partial pressure of 20 bar, which was accounted for separately. The compressor was modeled separately from the house load because the energy consumption calculated using ASPEN Plus was 500 kWh per Mg of gasified feedstock, which represents a significant fraction of the total energy consumption used to process the feedstock. Sensitivity of model results to compressor energy use is discussed in Section 3.6.

2.4. Fischer-Tropsch and refinement

FT product yields are estimated using the Anderson-Schulz-Flory (ASF) distribution equation, shown in Equation (3) (Spath and Dayton, 2003), along with the assumed CO conversion efficiency and syngas composition. The ASF equation estimates the weight distribution of carbon chain lengths. In this analysis, a chain growth probability, or α-value, of 0.95 is used to describe the FT reaction, which produces syncrude with a hydrocarbon distribution similar to crude oil (Claeys and van Steen, 2004). The modeled system includes two FT reactors in series to increase the CO conversion rate. The catalyst reacts 60% of the input CO in each reactor, so two reactors have a total reaction of 84% of initial CO (i.e., 60% in the first reactor and 60% of the unreacted 40% in the second reactor). The ASF carbon chain length weight fractions are then summed over the relevant carbon chain ranges shown in Table 3 to produce product weight fractions, which are combined with input mass (calculated from syngas composition) to estimate the unrefined product yield. The total syncrude yield is calculated using the total reformed syngas mass. Syncrude yield is assigned to individual waste fractions based on their contribution to total CO, similar to the CO_2 produced as a result of the water-gas shift reaction:

$$W_{\mathrm{n}} = n \cdot (1-\alpha)^2 \alpha^{\mathrm{n}-1} \tag{3}$$

where:

W_{n} weight fraction for carbon chain length n
α chain growth probability
n carbon chain length

For simplicity, gaseous hydrocarbons are assumed to be removed from the unrefined FT products. The gas is used to fuel a combustion turbine that generates electricity at 40% efficiency, which is used to offset grid electricity. In addition, heat is recovered during syngas cooling and from the exothermic FT reaction. The heat available from syngas cooling was estimated using ASPEN Plus, and the heat created from the FT reaction was calculated using reaction chemistry (Spath and Dayton, 2003). In this analysis, we assume that this generated heat, along with the heat recovered from gasification, can be converted into electricity via a steam cycle with a 30% thermal efficiency, which is also used to offset grid electricity. Though the model has the functionality to include further distillation onsite, it is assumed that all liquid hydrocarbons are transported to an existing petroleum refinery located offsite. RDF mass flow from a single facility produces a low volume of FT products compared to the throughput of a conventional petroleum refinery. As a result, construction of a full-scale refinery with its many energy intensive unit processes (e.g., distillation, hydrotreating) was not considered a cost-effective alternative (Pellegrino et al., 2007).

Using the NREL LCI database (2012), we estimate that the production and refinement of 1 kg of conventional petroleum requires 0.13 MJ of energy and releases 0.11 kg of CO_2e emissions. Our model equates 1 kg of liquid FT products (syncrude) with a kilogram of crude oil from the NREL database. Thus, FT and petroleum production are modeled with identical product distributions and fuel combustion emissions. Because FT products are low in sulfur and other impurities, refineries may bypass some purification processes, reducing the syncrude refinement energy consumption (Marano and Ciferno, 2001). Due to the small contribution of syncrude to the total refinery throughput; however, in the present analysis syncrude and fossil-based crude oil are assumed to undergo the same amount of refinement. Syncrude is transported

Table 3
Carbon chain length ranges for unrefined FT products (Source: Spath and Dayton, 2003).

Hydrocarbon type	Carbon-length range
Gaseous	1–4
Light liquid	5–11
Diesel	12–20
Heavy liquid	21–25
Solids	26+

250 km via truck to a coastal port followed by 2700 km of ocean freighter transport to a refinery. The refinery produces diesel, gasoline, liquefied petroleum gas (LPG), kerosene, residual fuel oil, refinery gas, bitumen, and petroleum coke from syncrude (NREL, 2012).

Refined products from both crude and syncrude are distributed together and assumed to have equal energy densities. However, there may be substantial differences in the GWP associated with the combustion of MSW derived FT products, depending on the biogenic fraction of MSW.

3. Model results

To quantify the energy and environmental performance of converting MSW to liquid fuels, we examined the mass flow, fuel yields, CED, energy production, and GWP based on an assumed input waste composition.

3.1. Mass flow

The RDF facility outputs include RDF, recyclable ferrous and aluminum, and a residual stream. Of the collected MSW mass, 54% is recovered as RDF and 2% as recyclable metals, with the remaining 44% being residual. As shown in Table 4, each material entering the RDF facility constitutes a different share of each RDF facility output. Recyclable paper and plastic make up 61% of the RDF.

3.2. Gasification

Using the calculated RDF composition, syngas yield is estimated per Mg of MSW, as shown in Table 5. Though 19% of RDF is of fossil origin, 36% of the produced syngas originates from fossil sources.

3.3. Fischer-Tropsch yields

The calculated syngas yield was used with ASF Equation (3) to estimate syncrude yield from the two FT reactors. Although the bulk of the electricity generation comes from waste heat recovery, a small amount of electricity can also be generated through the combustion of short-chain hydrocarbons produced by gasification and FT. We estimated that approximately 5.2 kg of gaseous hydrocarbons (with 4 or fewer carbon atoms) were generated during gasification and FT processing per Mg of solid waste. When these gaseous hydrocarbons were combusted, they produced 0.03 kWh of electricity, which contributed to the GWP associated with FT refinement. Syncrude constituted the remaining 223 kg of hydrocarbons produced by FT. LCI data for petroleum refining is given in Table 6. Note that for every 1 kg of syncrude entering the refinery, only 0.98 kg of refined product is created due to losses in the refining process. Thus, the refined product yields in Table 6 take into account the mass loss.

3.4. Energy consumption and production

Cumulative energy demand (CED) associated with material processing within the specified system boundary comes from electricity to power equipment and facilities, and fuel for transportation vehicles and rolling stock within the RDF facility. The system consumes 4.4 GJ of primary energy per Mg of MSW input. The energy content of the produced electricity and fuels for each Mg of MSW input following GFT is 10.8 GJ. Included in the 10.8 GJ is the heat recovered and used to generate 193 kWh of electricity produced in the GFT facility, which offsets grid electricity. As a result, the modeled system produces 2.4 (10.8/4.4) times as much energy as it consumes to convert the MSW feedstock into refined products. As shown in Fig. 3, the GFT facility consumes the most energy because of post-gasification syngas compression and the house load, which represent 68% and 12% of total process-related energy consumption, respectively.

3.5. Process-specific global warming potential

Emissions contributing to GWP result from process-related fuel and electricity consumption, GFT emissions, and FT fuel combustion. The net GWP of this system is −205 kg CO_2e per Mg MSW. This indicates that the GWP associated with the substituted conventional petroleum conversion and substituted grid electricity is larger in magnitude than the gross GWP associated with the FT system, as shown in Fig. 4. The emissions from energy entering the system boundary and GFT processes have a higher GWP than the offset pre-combustion emissions, which occur during the production of conventional petroleum derived fuels and products. However, FT fuel combustion has lower GWP than conventional fuels. Though both conventional petroleum-derived fuels and MSW-derived fuels have identical combustion emissions, the CO_2 derived from the biogenic RDF components does not contribute to GWP. Even though 81% of RDF is biogenic, the combustion

Table 4
Composition of RDF facility output streams. The RDF facility separates the national average input waste composition, derived from U.S. EPA (2011) and located in Table A3, into three streams with three different compositions.

	Composition of		
	RDF	Recycled metals	Residuals
Recyclable fiber	53%	0%	0%
Recyclable plastic	8%	0%	0%
Non-recyclable fiber	14%	0%	0%
Non-recyclable plastic	10%	0%	0%
Ferrous	0%	58%	0%
Aluminum	0%	42%	0%
Other organics	15%	0%	80%
Other inorganics	0%	0%	20%

Table 5
Syngas composition and yield. The calculated RDF composition is used to estimate syngas yield and composition.

	CO	H_2	CO_2	CH_4
Yield (10^3 mol/Mg MSW)[a]	8.3	16.6	9.3	0.0

[a] To convert the values in Table 5 to units of yield per mass of RDF, divide the values by 0.54, which is the fraction of MSW that becomes RDF.

Table 6
Fischer-Tropsch products. The estimated syncrude yield is combined with refined product yield data to predict FT products.

FT product	Yield (kg produced/ kg syncrude) (NREL, 2012)	Mass (kg produced/ Mg MSW)	Volume (L produced/ Mg MSW)
Diesel	0.22	48	57
Gasoline	0.41	92	123
Liquefied petroleum gas (LPG)	0.026	6	11
Kerosene	0.089	20	25
Residual fuel oil	0.048	11	12
Refinery gas	0.044	10	
Bitumen	0.036	8	
Petroleum coke	0.058	13	
Refining co-products	0.050	11	
Total	0.98	218	

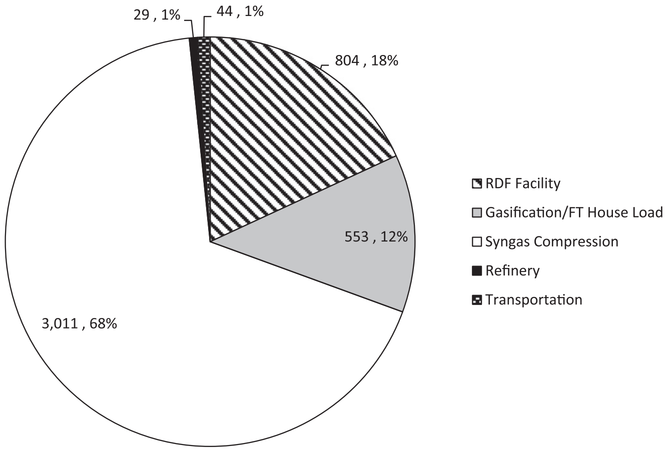

Fig. 3. Energy consumption by process within the system boundary. The first number label represents the energy consumption per unit mass (MJ/Mg MSW) followed by the share of cumulative energy demand within the system boundary. Syngas compression, required to achieve high FT conversion efficiencies, requires the largest share of energy.

emissions from FT fuels are only 64% less than conventional fuels because plastics generate more syngas and thus more fuel than biogenic components.

3.6. *Sensitivity analysis*

Model response to variations in input values was also explored. We performed a bounding analysis on waste composition by exploring large changes to fiber and plastics content. The percentage of fiber and plastic were each increased and decreased by 20% separately to create four new waste compositions. As each specified waste component was adjusted, the other waste components were scaled proportionally such that mass was conserved. For example, increasing fiber content resulted in a reduction in the plastic and organics content.

When fiber content, composed of biogenic carbon, is increased or plastic content is decreased, the net GWP decreases, as shown in Fig. 5. Because fiber has a lower syngas yield than plastic, waste compositions with higher fiber content produce less refined products than compositions with high plastic content. However, the lower gas volume associated with the higher fiber composition requires less air compression energy, and fiber is removed early in the RDF process, as shown in Appendix Fig. B1, both of which reduce the energy requirement and gross GWP from making fuels from fiber. In addition, fiber-derived fuels release biogenic CO_2 when combusted. Fig. 5 and Table 7 reveal that the difference in net GWP between the default composition and all the other waste compositions is within 11% of the initial gross emissions.

FT fuel yields vary less than 20% from the default waste composition fuel yield, as shown in Table 7. Across the different waste compositions, net GWP varies between −144 and −267 kg CO_2e. Although the net GWP values vary by a factor of 2, they are between 24% and 47% of the corresponding gross GWP value, as shown by the normalized net GWP in Table 7. Because FT product yield varies little between waste compositions, the net GWP divided by the total FT product mass follows trends similar to the net GWP.

Changes to input parameters can alter environmental impacts directly, by affecting energy consumption and direct emissions, or indirectly, by affecting FT yield and the resulting offsets. To analyze how input parameters can directly affect environmental impacts, we explored GWP sensitivity to the compressor electricity requirement, fraction of CO reacting in FT, number of FT reactors, and carbon intensity of grid electricity. The compressor electricity requirement was varied over a range from 50% lower to 50% greater than the default value of 500 kWh. The carbon intensity of grid electricity was varied from 0.28 to 0.67 kg CO_2e/kWh. The lower bound represents implementation of a CO_2 policy requiring a 50% decrease in the current electric sector carbon intensity, and the upper bound represents the average carbon intensity of electricity over the last half century based on U.S. EIA (2012). The GWP resulting from parameter variation, illustrated graphically in Fig. 6, revealed that the air compressor electricity requirement changed the net GWP linearly from −280 kg CO_2e at 50% of the initial value to −131 kg CO_2e at 150% of the initial value, which is much larger than the range of −187 to −250 kg CO_2e created by the carbon intensity of grid electricity. If carbon intensity decreases, changes to the compressor electricity requirement will cause smaller variations in net GWP.

In addition, to explore the effect of modifying fuel yield on GWP, we separately varied the fraction of CO reacting in each reactor and

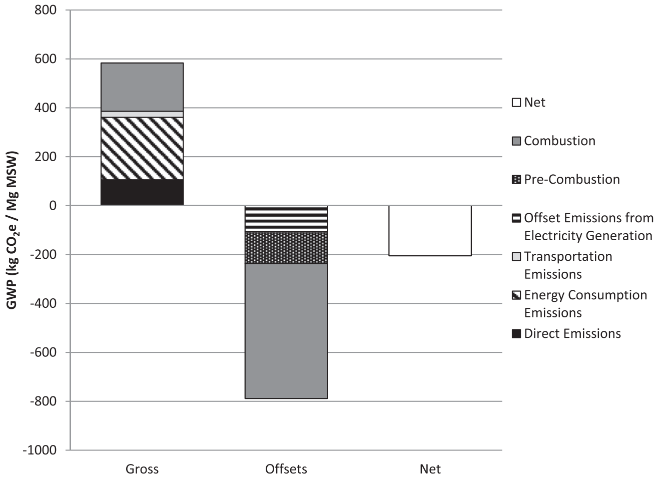

Fig. 4. GWP for the MSW conversion processes (RDF processing through syncrude refining) and the offsets associated with conventional petroleum processing. The net GWP represents the difference between gross emissions and the offsets for 1 Mg of MSW. Per IPCC guidelines (2007), biogenic CO_2 emissions (625 kg CO_2 per Mg of waste) are not included in the gross CO_2e estimate.

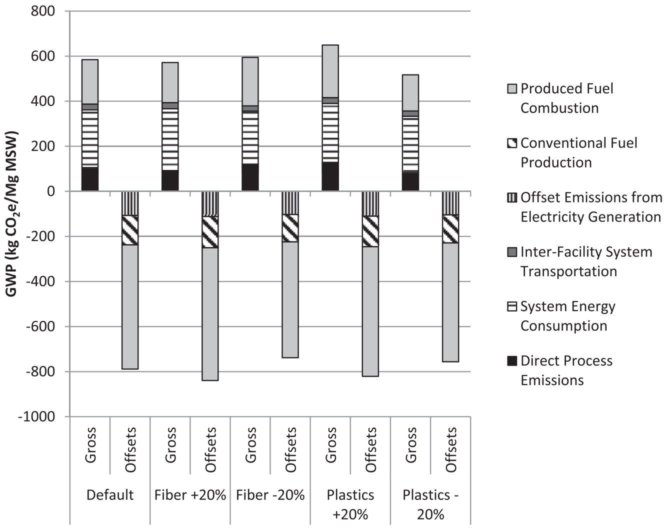

Fig. 5. GWP of multiple waste compositions. Variations in fiber and plastic content alter both the gross system and offset GWP. The net GWP for each scenario is given in Table 7.

Table 7
GWP and syncrude yield for multiple waste compositions. Varying waste composition changes GWP and syncrude yield.

Waste composition	Net GWP (kg CO_2e)	Total FT product mass (kg)	Net GWP/ Mass FT product (kg CO_2e/kg product)	Normalized net GWP (fraction of gross GWP)[a]
Default	−204	220	−0.93	−0.35
Fiber +20%	−267	230	−1.16	−0.47
Fiber −20%	−144	200	−0.72	−0.24
Plastics +20%	−172	230	−0.75	−0.26
Plastics −20%	−239	210	−1.14	−0.46

[a] For example, this value is calculated as −204/585 for the default case.

the number of reactors from 50% to 150% of the initial values of 0.6 and 2, respectively. Both parameters display a negative exponential relationship with net GWP because the total CO reacting is calculated with an exponential function that uses the fraction of CO reacting in each reactor and the number of reactors. Since neither parameter is associated with energy consumption, the GWP effects are directly related to the fuel yield. The fraction of CO reacting had a net GWP range of −61 to −271 kg of CO_2e, larger than the range from varying the number of reactors. However, the benefit of adding reactors should not be overlooked since it is simpler to add a reactor than redesign the entire system to achieve a higher CO reaction rate.

4. Discussion

The treatment of 1 Mg of MSW via material sorting, gasification, and FT to create liquid fuels comparable to conventional refined petroleum products and electricity generation results in a net GWP that is small compared to the gross and offset GWP (Fig. 4). A large share of the CED associated with MSW conversion to liquid fuels is related to the compressor requirement for FT. Sensitivity analysis indicates that if CO yields have been significantly overestimated, liquid fuels produced from MSW can have a GWP comparable to conventional petroleum.

In addition, the model results indicate that changing MSW composition alters the net GWP. Plastics and fiber are the predominant RDF components, so variation in each was explored. Plastics were found to have higher syngas yields, in both the ASPEN Plus and the spreadsheet model, which led to higher FT fuel yields than fiber. However, plastics have a GWP equivalent to conventional petroleum products given their origin as conventional petroleum. The net effect is that RDF with higher plastics content results in higher GWP because the higher combustion emissions outweigh the larger offsets obtained with higher fuel yields.

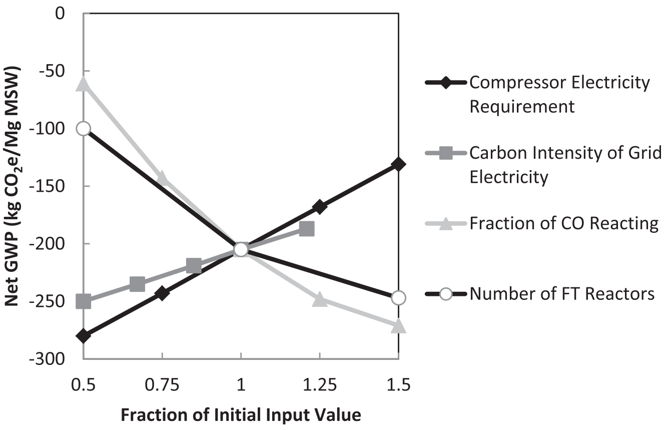

Fig. 6. Change in net GWP as a function of several key model parameters.

Further analysis is required to quantify the effects of specific MSW policies on GWP, but model results suggest that removing plastics from MSW, via a recycling policy, would increase the environmental benefits of FT fuels at the expense of fuel yield. Because recycling fiber can produce positive or negative net GWPs depending on LCA system boundaries and the particular remanufacturing process (Merrild et al., 2008), changes in fiber recycling rates can result in an increase or decrease in GWP. Parametric sensitivity analysis of the air compression energy requirement, carbon intensity of electricity, CO reacting percentage, and number of FT reactors was used to quantify their effects on GWP. Because syngas compression accounts for 68% of the total energy consumption, we explored the effect of altering the compression electricity requirement. If more compression is required to get the partial pressures of CO and H_2 into acceptable ranges, the energy requirement will increase. However, the energy requirement could decrease if advances in FT technology allowed for partial pressure requirements to decrease without affecting product yield. In the case where the compression energy requirement decreased 50%, the cumulative energy demand decreased by 34% to 2.93 GJ/Mg. An alternative approach is to operate the gasifier under pressurized and/or oxygen fed conditions. The limited scale of MSW gasifiers, however, may not justify the use of such gasification systems given their higher investment cost.

FT yield is most affected by the fraction of CO reacting and the number of FT reactors in series in the model, for a given α-value. The fraction of CO reacting affected yield more than the number of FT reactors, as shown in Fig. 6. However, if the fraction of CO reacting per FT reactor is low, increasing the number of reactors can be used to increase the total fraction of CO reacting. Once a FT system is fully-operational, adjusting the number of reactors may be more practical than altering the components of the FT system to increase FT fuel yield.

The gasification and FT system's GWP may also be affected by changes to the national energy system. If the carbon intensity associated with grid electricity decreases, the energy consumption GWP will decrease as shown in Fig. 6, since the overall process is a net electricity consumer. However, if the market share of biofuels increases, the GWP associated with the MSW-derived fuel will increase because combustion emission offsets will be less. On the other hand, it is possible that a move towards liquid transportation fuels derived from oil shale or oil sands with significantly higher GWP would result in a proportional reduction in the GWP of MSW-derived fuel. Such exogenous factors can affect the overall environmental performance of the system, and further analysis is needed to determine how changes to the broader energy system would affect the GWP of the studied system.

To compare an MSW system with GFT to conventional MSW systems, the system boundaries must be expanded to include curbside MSW collection, metals remanufacture, and residual treatment, which are not included in this analysis. Though future work will compare complete MSW management systems with consistent waste compositions and LCI data, a high-level comparison of how the results from this study compare with previously published studies can provide insight into the viability of GFT as an MSW treatment method. The calculated net GWP for the GFT system presented in this study is comparable to the −250 kg CO_2e/Mg for MSW in a state-of-the-art landfill and less than the 26 kg CO_2e/Mg for MSW in a national average landfill presented in Levis and Barlaz (2011). Harrison et al. (2000) assembled a LCI for a conventional waste-to-energy (incineration) system, which estimates the net GWP to be −260 kg CO_2e/Mg using IPCC (2007). The systems compared to this study begin with MSW delivered at the treatment facility (i.e., no collection). If RDF residual, which includes food waste, is landfilled, then the net GWP of the GFT system will increase (Levis and Barlaz, 2011). Though these studies include differing assumptions that make direct comparison with our study difficult, the GWP results nonetheless indicate that GFT technology falls within a similar range as alternative MSW treatment methods.

Acknowledgments

The authors would like to acknowledge support from the Biofuels Center of North Carolina (gs1) and the Environmental Research and Education Foundation (EREF (gs2)), which made this work possible.

Appendix A. Supplementary Material

Supplementary data related to this article can be found online at http://dx.doi.org/10.1016/j.jclepro.2014.02.041

References

Ahmed, I., Gupta, A.K., 2009. Evolution of syngas from cardboard gasification. Appl. Energ. 86, 1732–1740.

Ahmed, I.I., Nipattummakul, N., Gupta, A.K., 2011. Characteristics of syngas from co-gasification of polyethylene and woodchips. Appl. Energ. 88, 165–174.

Ammendola, P., Chirone, R., Miccio, F., Ruoppolo, G., Scala, F., 2011. Devolatilization and attrition behavior of fuel pellets during fluidized-bed gasification. Energ. Fuels 25, 1260–1266.

Arafat, H.A., Jijakli, K., 2013. Modeling and comparative assessment of municipal solid waste gasification for energy production. Waste Manag. 33, 1704–1713.

Aspen Technology Inc, 2010. ASPEN Plus v7.2 User Model. Aspen Technology, Inc, Cambridge, MA.

Belgiorno, V., De Feo, G., Della Rocca, C., Napoli, R.M.A., 2003. Energy from gasification of solid wastes. Waste Manag. 23, 1–15.

Cao, Y., Gao, Z., Jin, J., Zhou, H., Cohron, M., Zhao, H., Liu, H., Pan, W., 2008. Synthesis gas production with an adjustable H_2/CO ratio through the coal gasification process: effects of coal ranks and methane addition. Energ. Fuels 22, 1720–1730.

Carpentieri, M., Corti, A., Lombardi, L., 2005. Life cycle assessment (LCA) of an integrated biomass gasification combined cycle (IBGCC) with CO_2 removal. Energ. Convers. Manag. 46, 1790–1808.

Christensen, T.H., Gentil, E., Boldrin, A., Larsen, A.W., Weidema, B.P., Hauschild, M.Z., 2009. C balance, carbon dioxide emissions and global warming potentials in LCA-modelling of waste management systems. Waste Manag. Res. 27, 707–715.

Claeys, M., van Steen, E., 2004. Basic studies. In: Fischer-Tropsch Technology, Studies in Surface Science and Catalysis. Elsevier B.V.

Cyclo-Tempo, 2012. A Program for Thermodynamic Modeling and Optimization of Energy Conversion Systems. Delft University of Technology [online]. http://www.cycle-tempo.nl/. Updated 2 December 2012. [Cited 5 July 2013].

Ecoinvent, 2010. Ecoinvent Data V2.2. Swiss Centre for Life Cycle Inventories.

Energy Centre of the Netherlands, 2012. Phyllis2 [online]. http://www.ecn.nl/phyllis2/. Updated 2012. [Cited 5 July 2013].

European Commission, March 2010. European Commission – Joint Research Centre – Institute for Environment and Sustainability. EUR 24708 EN, first ed.. In: International Reference Life Cycle Data System (ILCD) Handbook – General Guide for Life Cycle Assessment – Detailed Guidance Publications Office of the European Union, Luxembourg.

Flory, P.J., 1936. Molecular size distribution in linear condensation polymers. J. Am. Chem. Soc. 58, 1877–1885.

Fock, F., Thomsen, K.P.B., Houbak, N., Henrikson, U., 2000. Modelling a biomass gasification system by means of "EES". In: Scandinavian Simulation Society. Presented at the SIMS 2000 Conference, Kgs. Lyngby, Denmark.

Gai, C., Dong, Y., 2012. Experimental study on non-woody biomass gasification in a downdraft gasifier. Int. J. Hydrog. Energ. 37, 4935–4944.

Harrison, K.W., Dumas, R.D., Barlaz, M.A., Nishtala, S.R., 2000. A life-cycle inventory model of municipal solid waste combustion. J. Air Waste Manag. Assoc. 50, 993–1003.

Hirst, E., 1974. Food-related energy requirements. Science 184, 134–138.

IPCC, 2007. In: Solomon, S., Qin, D., Manning, M., Chen, Z., Marquis, M., Averyt, K.B., Tignor, M., Miller, H.L. (Eds.), Contribution of Working Group I to the Fourth Assessment Report of the Intergovernmental Panel on Climate Change. Cambridge University Press.

ISO, 2006a. ISO 14040: Environmental Management – Life Cycle Assessment – Principles and Framework. ISO, Geneva.

ISO, 2006b. ISO 14044: Environmental Management – Life Cycle Assessment – Requirements and Guidelines. ISO, Geneva.

Kaplan, P.O., DeCarolis, J., Thorneloe, S., 2009. Is it better to burn or bury waste for clean electricity generation? Environ. Sci. Technol. 43, 1711–1717.

Khoo, H.H., 2009. Life cycle impact assessment of various waste conversion technologies. Waste Manag. 29, 1892–1900.

Koehler, A., Peyer, F., Salzmann, C., Saner, D., 2011. Probabilistic and technology-specific modeling of emissions from municipal solid-waste incineration. Environ. Sci. Technol. 45, 3487–3495.

Lee, S., Loyalka, S.K., Speight, J.G., 2007. Handbook of Alternative Fuel Technologies. CRC Press, Boca Raton.

Levis, J.W., Barlaz, M.A., 2011. Is biodegradability a desirable attribute for discarded solid waste? Perspectives from a national landfill greenhouse gas inventory model. Environ. Sci. Technol. 45, 5470–5476.

Marano, J.J., Ciferno, J.P., 2001. Life-Cycle Greenhouse-Gas Emissions Inventory for Fischer-Tropsch Fuels. National Energy Technology Laboratory, U.S.Department of Energy.

Matuszewsk, M., Woods, M., 2012. QGESS: Process Modeling Design Parameters. NETL/DOE-341/081911, 2012. National Energy Technology Laboratory, U.S.Department of Energy. NETL/DOE-341/081911.

Ménard, J.-F., Lesage, P., Deschênes, L., Samson, R., 2004. Comparative life cycle assessment of two landfill technologies for the treatment of municipal solid waste. Int. J. LCA 9, 371–378.

Merrild, H., Damgaard, A., Christensen, T.H., 2008. Life cycle assessment of waste paper management: the importance of technology data and system boundaries in assessing recycling and incineration. Resour. Conserv. Recyl. 52 (12), 1391–1398.

Muñoz, I., Rigarlsford, G., Canals, L.M., King, H., 2012. Accounting for greenhouse gas emissions from the degradation of chemicals in the environment. Int. J. Life Cycle Assess. 18, 252–262.

National Renewable Energy Laboratory, 2012. U.S.Life-Cycle Inventory Database V1.1.

Nuss, P., Bringezu, S., Gardner, K.H., 2012. Waste-to-materials: the longterm option. In: Karagiannidis, A. (Ed.), Waste to Energy, Green Energy and Technology. Springer, London, pp. 1–26.

Nuss, P., Gardner, K.H., Jambeck, J.R., 2013. Comparative life cycle assessment (LCA) of construction and demolition (C&D) derived biomass and U.S. Northeast forest residuals gasification for electricity production. Environ. Sci. Technol. 47, 3463–3471.

Pellegrino, J., Brueske, S., Carole, T., Andres, H., 2007. Energy and Environmental Profile of the U.S. Petroleum Refining Industry.

Portofino, S., Donatelli, A., Iovane, P., Innella, C., Civita, R., Martino, M., Matera, D.A., Russo, A., Cornacchia, G., Galvagno, S., 2013. Steam gasification of waste tyre: influence of process temperature on yield and product composition. Waste Manag. 33, 672–678.

Pytlar, T.S., 2010. Status of existing biomass gasification and pyrolysis facilities in North America. In: Presented at the 18th Annual North American Waste-to-Energy Conference.

Riber, C., Bhander, G.S., Christensen, T.H., 2008. Environmental assessment of waste incineration in a life-cycle-perspective (EASEWASTE). Waste Manag. Res. 26, 96–103.

RTI International, 2012. Environmental and Economic Analysis of Emerging Plastics Conversion Technologies.

Ruoppolo, G., Ammendola, P., Chirone, R., Miccio, F., 2012. H2-rich syngas production by fluidized bed gasification of biomass and plastic fuel. Waste Manag. 32, 724–732.

Shabbar, S., Janajreh, I., 2013. Thermodynamic equilibrium analysis of coal gasification using Gibbs energy minimization method. Energy Convers. Manag. 65, 755–763.

Spath, P.L., Dayton, D.C., 2003. Preliminary Screening – Technical and Economic Assessment of Synthesis Gas to Fuels and Chemicals with Emphasis on the Potential for Biomass-derived Syngas.

Sreejith, C.C., Muraleedharan, C., Arun, P., 2012. Equilibrium modeling and regression analysis of biomass gasification. J. Renew. Sust. Energy 4, 063124.

Swain, P.K., Das, L.M., Naik, S.N., 2011. Biomass to liquid: a prospective challenge to research and development in 21st century. Renew. Sust. Energ. Rev. 15, 4917–4933.

U.S. EIA (United States Energy Information Administration), 2012. Annual Energy Review 2011. Office of Energy Statistics. DOE/EIA-0384(2011).

U.S. EPA (United States Environmental Protection Agency), 2011. Municipal Solid Waste Generation, Recycling, and Disposal in the United States. In: Facts and Figs for 2010.

Vera, D., de Mena, B., Jurado, F., Schories, G., 2013. Study of a downdraft gasifier and gas engine fueled with olive oil industry wastes. Appl. Therm. Eng. 51, 119–129.